Amplification of microchip oscillator emission using a diode-pumped wedged-slab amplifier

Jeffrey G. Manni *

JGM Associates, Inc., 25 Burlington Mall Road, Suite 300, Burlington, MA 01803, USA

Received 19 January 2005; received in revised form 25 March 2005; accepted 25 March 2005

Abstract

A master-oscillator power-amplifier (MOPA) system combines a 1064-nm microchip laser oscillator with a new diode-side-pumped Nd:YVO_4 zig-zag slab amplifier design. With 40 W of diode pump power, the amplifier increases microchip average power from 200 mW to more than 2.5 W at a 10-kHz pulse rate for a single pass through the amplifier, and to 5.7 W for two-passes, while preserving microchip laser beam quality and emission spectrum. Pulse energy of more than 800 1J was achieved at a 2-kHz pulse rate. These results are the highest reported to date in an amplified microchip laser system. The 15-mm-long Nd:YVO_4 slab has thin-film-coated lateral sides that enable a zig-zag gain length longer than 5.5 cm for a single pass through the slab, which is the longest reported to date. The unique slab design has non-parallel or wedged lateral sides to prevent build-up of amplified spontaneous emission. The two-pass beam is separated from the input beam without using a Faraday device.

1. Introduction

Microchip lasers are ultra-compact sources of single-frequency emission that can achieve pulse durations substantially less than 1 ns, peak power levels in excess of 10 kW, kilohertz pulse repetition rates, and pulse energies of a few microjoules, pumping with only 2 W of continuous-wave diode pump power [1]. The inventor of the microchip la- ser, J.J. Zayhowski, has published extensively on the topic of microchip laser design and applica- tions. Envisioned applications include range-re- solved remote imaging and sensing, pumping of optical parametric generators, oscillators, and amplifiers that employ periodically poled nonlin- ear materials, UV generation, micromachining and microsurgery, and laser-ionization breakdown spectroscopy [2]. Microchip laser products are now commercially available from JDS Uniphase (San Jose, CA).

* Tel.: +1 7812726692; fax: +1 7812217154.
E-mail address: jgmanni@jgma-inc.com.

Microchip laser sources that provide higher pulse energy and average power without compromising single-frequency or TEMoo performance are desirable for many existing and envisioned applications, especially if nonlinear wavelength conversion processes are needed to obtain the desired wavelength(s). Zayhowski has described microchip oscillator designs that scale output energy to as much as 250 μJ per pulse, and recently reported on a patented microchip oscillator-amplifier design in which pump energy not absorbed in the microchip oscillator is used to pump a tandem microchip amplifier [3,4].

Other schemes for amplifying microchip laser emission have also been reported. Druon et al. [5] amplified microchip emission to 11 μJ at a 45-kHz pulse rate. Isyanova et al. [6] used a diode-pumped Nd:YVO_4 slab amplifier in a double-pass configuration to amplify 3.5 μJ pulses from a microchip Nd:YAG laser to more than 300 μJ energy at a 2-kHz pulse rate (more than 700 mW average power). Two 20 W diode bars were used to side-pump the slab amplifier. Amplified emission was single-frequency and had near-TEMoo beam quality. A Faraday isolator was used to separate the two-pass-amplified output beam from the input beam, and a recirculating-water chiller cooled the diode-pumped amplifier.

Kliner et al. [7] mated a microchip laser oscillator to a Yb-doped fiber amplifier pumped with 3 W of 976 nm diode power. The microchip laser provided 40 mW of 1064-nm average power at a pulse rate of about 4 kHz, which was amplified to 320 mW of TEMoo emission by the fiber amplifier.

This paper describes a novel high-gain diode-pumped Nd:YVO_4 slab amplifier that achieves substantially improved amplifier extraction efficiency and average output power compared to previously reported microchip MOPA designs.

2. Microchip laser

The microchip laser used in these experiments was fabricated using an epoxyless crystal-bonding method developed by VLOC (New Port Richey, FL). The microchip was fabricated, bonded, and coated by VLOC.

The microchip laser design used here represents an attempt to achieve pulse energy of 10 μJ or more, and pulse duration longer than 1 ns, while maintaining the extreme compactness and simplicity of a microchip oscillator design. The microchip consisted of a 3-mm-long Nd^{3+}:YAG section (1% atomic Nd) and a 2.2-mm Cr^{4+}:YAG section. Prior to bonding, the uncoated Cr^{4+}:YAG section had a small-signal transmission of 50% at 1064 nm, including Fresnel reflection losses of the uncoated crystal. After bonding, the Nd:YAG or pumped end face of the microchip was coated for high transmission (HT) at 808 nm and high reflectivity (HR) at 1064 nm. The Cr:YAG or output face of the microchip was coated HT at 808 nm and 60%R at 1064 nm. The finished microchip laser was 3 by 3 mm in cross-section and had an overall physical length of 5.2 mm. An off-the-shelf mount held the chip by its top and bottom surfaces under slight compression. Indium foil was placed between the chip and each mounting surface.

The microchip was optically pumped using the setup shown in Fig. 1. The pump diode was a fiber-coupled single-emitter diode laser (Coherent) that provided up to 2.5 W of cw 808 nm power (3 nm bandwidth) through a 200-μm-core, 0.22 NA fiber. A lens pair acting as a non-imaging concentrator reduced the pump spot at the microchip

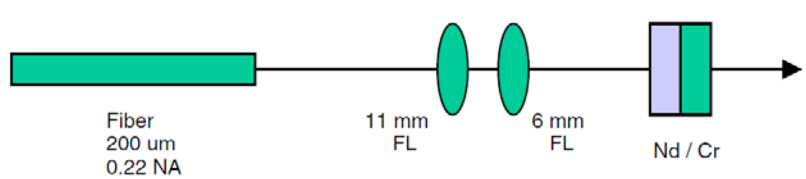

Fig. 1. Microchip pumping scheme.

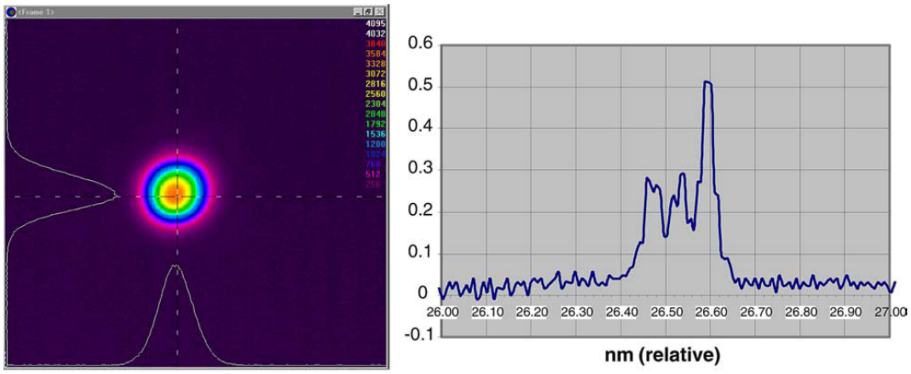

Fig. 2. (Left) Microchip laser beam profile, and (right) microchip laser emission spectrum.

to about 110 μm; the pump NA external to the microchip increased to about 0.4.

The microchip laser produced 200 mW of average power at a 10-kHz pulse rate when pumped with 2.0 W of cw power. The measured pulse width was 1.0–1.2 ns FWHM. The microchip spatial beam profile is shown in Fig. 2. The beam was collimated with a 50-mm FL lens and the spatial beam profile was measured about 40 cm from the collimator lens. Beam diameter (13.5% of peak) versus distance data were recorded through a beam waist created with a 100-mm FL lens. The fitted M^2 values were $M_x^2 = 1.00$ and $M_y^2 = 1.04$.

The microchip laser's emission spectrum, integrated over many pulses, is also shown in Fig. 2. The spectrum was not single-frequency, but instead consisted of three modes spaced 0.06 nm apart. No attempt was made to optimize the microchip design for true single-frequency operation. (Each pulse is probably single-frequency, but, when operating at 10 kHz, the longitudinal mode that lases "hops" between the three modes shown on a pulse-to-pulse basis).

3. VHGM amplifier

The author has designed a novel diode-side-pumped, zig-zag slab amplifier that achieves high gain-per-pass by employing Nd:YVO_4 as the gain medium, and by enabling long single-pass gain lengths (4–6 cm) using a slab only 15 mm long. A first prototype of this amplifier has been built and tested, and results are reported here publicly for the first time. The amplifier is referred to below as the very high gain module (VHGM).

Fig. 3 shows the basic VHGM design. A rectangular slab of laser gain material is side-pumped by diode laser bars from one or both sides. The bars have microlenses to collimate pump emission in the fast-axis direction.

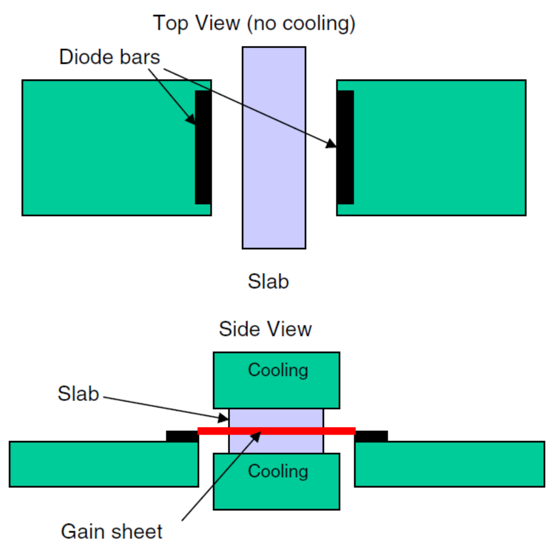

Fig. 3. VHGM layout.

The diode bars may be positioned close to the side of the slab (1 mm or less), or more than 20 mm away, depending on packaging constraints, residual fast-axis beam divergence, and other design considerations.

All VHGM experiments to date have been conducted with an $Nd:YVO_4$ slab. Typical slab dimensions are 2 mm thick by 15 mm long by 4–6 mm wide. A thin "gain sheet" is created in the slab by arranging that diode pump light be absorbed in fairly uniform fashion across the width of the slab, but not so uniformly that excessive unabsorbed power exits the opposite side of the slab. In general, diode pump wavelength, pump light polarization, and dopant concentration are adjusted to achieve the desired tradeoff between pumping uniformity and pump-light absorption/laser output efficiency.

Nominal dimensions of the gain sheet so formed are 1 cm long (a typical diode bar length), by 0.3–1 mm thick (depending on the microlens used to fast-axis-collimate the diode bars), by 3–6 mm wide, depending on the width of the laser slab.

The slab is conductively cooled at its top and bottom surfaces. A layer of indium foil or solder establishes good thermal contact between the slab and cooling surfaces. The symmetry of the cooling boundary conditions creates thermal and refractive index gradients with rectangular symmetry, thereby facilitating amplification of plane-polarized beams polarized parallel or perpendicular to the thermal gradient.

The slab can be pumped with quasi-cw or cw diode bars of virtually any power level, including commercially available 20, 40, 60, and 80 W cw bars. In theory, side-pumping and distribution of absorbed pump light along the width of the slab allows pumping with more than 150 W of total average or cw power without fracturing the $Nd:YVO_4$ slab. This situation enables high-average-power as well as high-gain laser amplifiers and oscillators that incorporate VHGMs.

The diode bars can be placed within a few millimeters of the slab, or up to 20 or 30 mm away, assuming that diode bar emission is reasonably well collimated in the fast axis. In general, each diode bar is placed far enough away that the individual diode beamlets are well overlapped in the slow-axis plane as they enter the slab. Because the diode bars can be far away, 2D-array pumping schemes are also possible in which intervening optics are used to reduce fast-axis pitch between the multiple 1D array beams.

The "lateral" sides of the slab, through which diode pumping occurs, have thin-film dichroic coatings highly reflecting (HR) at the laser wavelength and highly transmitting (HT) at the diode pump wavelength. These HR/HT coatings are patterned to provide entrance and exit windows on the lateral sides for the laser beam being amplified. The slab is fabricated with a substantial wedge angle between the two lateral sides, and this wedge angle is selected to prevent buildup of parasitic amplified spontaneous emission (ASE) over the range of intended pump power levels. In addition, one or both end faces of the slab are canted to prevent ASE buildup.

Fig. 4 shows typical zig-zag beam paths through the VHGM slab. Depending on the input beam's angle of incidence, the lateral wedge angle in the slab, and the HR/HT coating pattern, the output beam can be made to exit the slab on the same side as the input beam or on the opposite side.

The number of bounces on the lateral sides is controlled by adjusting the input beam's angle of incidence. There is no need to match bounce points of the zig-zag path to diode-bar emitter positions, as in Baer's "tightly folded resonator" design [8]. In fact, it is not possible to do such matching (assuming the diode bars have uniform emitter pitch) considering that the bounce points are spaced non-uniformly along the lateral sides of the wedged VHGM slab. Furthermore, the diode beamlets are typically well overlapped in the zig-zag plane as they enter the slab, so there are no well-defined pump beamlets in the slab as in Baer's design.

The diameter of the laser beam being amplified is adjusted so its vertical dimension in the slab (perpendicular to the zig-zag plane) is nominally equal to the thickness of the gain sheet. The input beam can also be focused in the vertical direction so the beam is smaller than the gain sheet thickness at some points along the zig-zag path. The horizontal diameter of the input beam (in the zig-zag

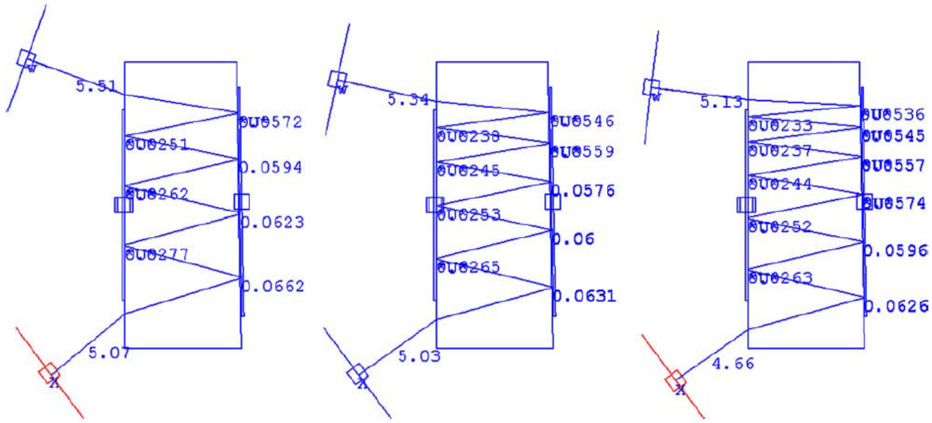

Fig. 4. Zig-zag paths for different incident beam angles.

plane), and the number of bounces, are adjusted so the beam efficiently extracts energy stored in the gain sheet, but without significant beam clipping at coating or crystal edges. This scheme is well suited to amplifying TEMoo laser beams.

With a 15-mm long $Nd:YVO_4$ slab, and slab widths of 4–6 mm, single-pass gain lengths of 40–60 mm can be achieved by adjusting the input beam angle. Such long single-pass gain lengths would be difficult if not impossible to achieve using total internal reflection to configure the zig-zag beam path. Single-pass unsaturated gains in excess of 100,000 are achievable considering that unsaturated gain coefficients of 1–2 cm^{-1} are possible when pumping $Nd:YVO_4$ with 20–40 W diode bars.

In the VHGM, the zig-zag beam path reflects off the same lateral surfaces through which optical pumping occurs. Therefore, the "zig-zag averaging effect" acts to mitigate the effects of diode-pumping and other optical non-uniformities that occur in the zig-zag plane. For the VHGM, the in-plane non-uniformities are due primarily to absorption/attenuation of pump light in the slab, and, to a lesser extent, to relatively weak thermally induced optical effects that occur in the zig-zag plane. Because the VHGM slab is cooled at the top and/or bottom slab surfaces, a strong thermal gradient exists perpendicular to the zig-zag plane under high-average-power pumping conditions. Optical effects of this vertical gradient (e.g., thermal lensing) are not averaged by the zig-zag beam path, and must be considered when designing VHGMs into oscillator and amplifier systems. However, as long as the beam being amplified has a polarization in or perpendicular to the zig-zag plane, plane-polarized beams can be amplified without significant degradation of polarization ratio or beam quality.

Since the zig-zag beam path reflects off the same surfaces through which diode pump light is injected (active mirror design), the strength of pump light absorption in the slab can be adjusted over a fairly wide range without significantly affecting beam quality or laser efficiency, at least for high-gain four-level lasers such as $Nd:YVO_4$. The zig-zag beam path effectively overlaps pumped regions of the slab even if much of the pump light is absorbed within 1 or 2 mm from lateral side through which pump light enters. Preliminary data indicate that diode and $Nd:YVO_4$ slab temperature can be varied over a considerable range (e.g., 20 °C) without large changes in amplifier output power or beam quality.

4. Multi-passing VHGM amplifiers

VHGM-based amplifiers can, in principle, be two-passed, three-passed, and four-passed using geometric methods alone to separate the multi-pass beam from the input beam. Beam paths were

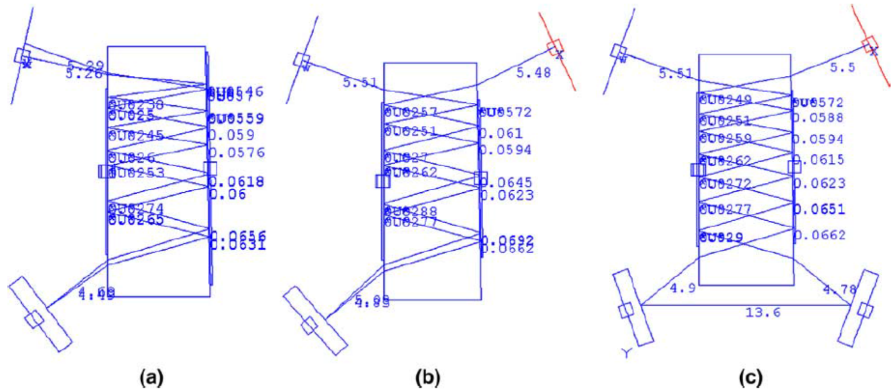

Fig. 5. Double-pass schemes using geometric methods alone to separate input/output beams.

modeled using Laserwerks optical modeling software (OptikWerk; Rochester, NY). Fig. 5 shows possible two-pass schemes that use external mirrors to send the beam back into the VHGM for a second pass. (In all parts of Fig. 5, the amplified beam enters at the upper left corner of the slab). In part (a), the two-pass beam exits at a different angle, so that, if placed far enough from the slab, a pickoff mirror can extract the two-pass beam. In parts (b) and (c), the two-pass beam is made to exit on the opposite side of the slab by adjusting the input angle for the second pass.

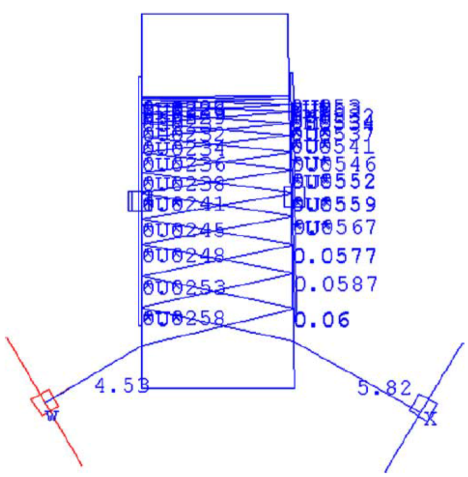

Fig. 6. Two-pass amplifier injecting the beam so it propagates initially toward the narrower end of the laterally wedged slab.

Fig. 6 shows another possible two-pass scheme with no external mirrors. The input beam is injected propagating toward the narrower end of the laterally wedged slab. By controlling input angle, the beam can be made to reverse direction at some point within the slab, and then emerge on the same end but opposite side of the slab after making a second pass. Another scheme is possible (not shown) in which the beam makes a total internal reflection off the far end face of the slab, which must be perpendicular to the zig-zag plane, to make a second pass through the gain sheet.

The two-pass schemes shown above enable total gain lengths of 8–12 cm in a Nd:YVO_4 slab that is 15 mm long by 3–6 mm wide, without using a Faraday isolator to separate input and output beams. Three-pass and four-pass schemes are also possible which start with one of the two-pass schemes shown above, and then reflect the beam back into the VHGM for more passes using additional mirrors as required. Especially for three- or four-passing, lenses placed between the slab and external mirrors may be needed to control horizontal and vertical beam diameters so as to improve mode matching or prevent beam clipping.

5. Compatible gain media

Although high laser gains are achieved easily with Nd:YVO_4, high-gain VHGM designs can be realized with other types of laser gain media, especially ones for which slabs much longer than 15 mm can be obtained. Examples include Nd:YAG, Nd:YLF, and Nd:YALO.

High pump power densities are possible in VHGM slabs because high pump power levels can be used without fracturing the slab, and because the gain sheet can be made relatively thin (e.g., less than 0.5 mm) without complicating spatial overlapping of the TEMoo beam being amplified with the gain sheet. Due to the high pump power densities that can be achieved, it should be possible to use VHGMs with quasi-three-level laser materials such as Yb:YAG, for which high pump density is needed to overcome reabsorption losses.

VHGMs may also be used with lower-gain laser materials. In this case, the combination of high pump power density and long zig-zag path lengths may render some lower-gain laser materials practical for amplifier applications that would otherwise not be.

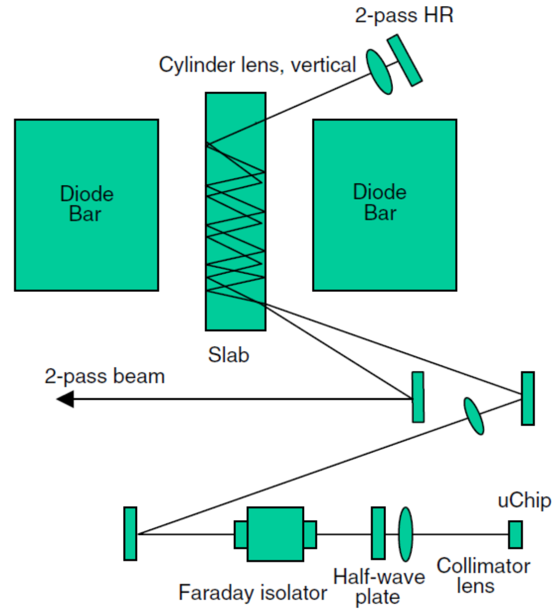

Fig. 7. Two-pass VHGM amplifier setup.

6. One-pass $Nd:YVO_4$ amplifier performance

The one-pass amplifier setup eliminates the "2-pass HR" mirror shown below in the Fig. 7. Microchip oscillator emission is collimated with a 50-mm FL spherical lens. The isolator is not necessary for 1-pass amplifier operation, but it facilitates switching between 1-pass and 2-pass configurations. The polarization state after the isolator is vertical to the plane of the paper. The half-wave plate adjusts beam polarization going into the isolator. All mirrors are flat HRs at 1064 nm.

Diode pump emission is polarized perpendicular to diode junction plane, or parallel to the *c*-axis of the $Nd:YVO_4$ slab. Peak diode wavelength is nominally 805 nm at 25 °C. The diode bars and slab are conductively cooled; there is no water flow through the diode cases or the slab mount. For these experiments, the diode bars and slab assembly sit on a water-cooled cold plate. Diode bars are electrically insulated from the cold plate using thermally conductive insulator pads.

The $Nd:YVO_4$ slab is 6 mm wide and 15 mm long and has a 1° lateral wedge angle. The Nd-doping level is 0.5% (atomic). The length of the zig-zag beam path that overlaps the nominally 10 mm long gain sheet is about 5.5 cm. A 100-mm FL cylinder lens is placed after the slab to recollimate the vertical axis of the output beam.

The microchip oscillator generates an average power of 200 mW at a 10-kHz pulse rate when pumped with 2 W of cw pump power. For the configuration shown, microchip laser power transmitted after one zig-zag pass through the slab was 160 mW, with the amplifier's pump diodes off. Transmission losses were due to Fresnel reflection losses at the four uncoated cylinder lens surfaces, and partially due to 1064 nm absorption in the $Nd:YVO_4$ slab. Microchip beam diameter at the slab (without the cylinder lens) was about 800 μm.

Fig. 8 shows the measured *L–I* curve for the 1-pass amplifier, pumping with a maximum of 20 W/bar or 40 W of total diode pump power at 36 A. Maximum amplifier output power was 2.6 W at a pulse rate 10 kHz, or 260 μJ per pulse. This is, to the best our knowledge, the highest reported average power and pulse energy from a microchip MOPA laser system using one single-pass amplifier stage.

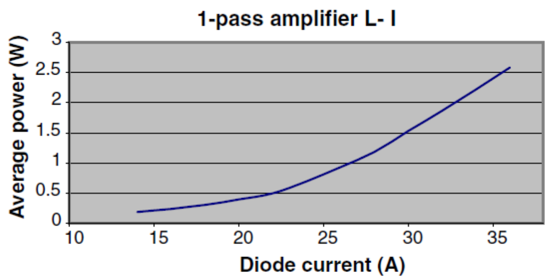

Fig. 8. One-pass VHGM amplifier *L–I* curve.

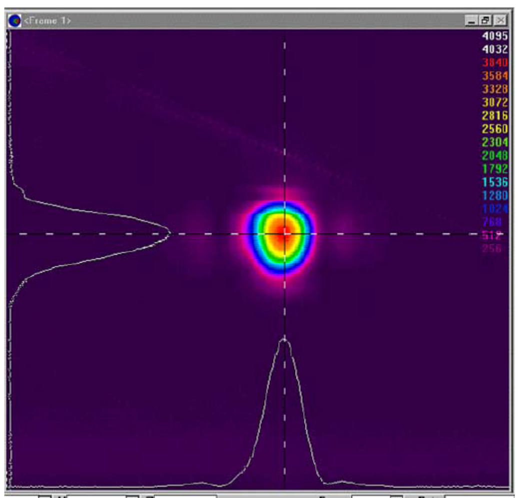

Fig. 9. One-pass amplifier beam profile, 2.6 W at 10 kHz.

Fig. 9 shows a spatial profile for the 1-pass output beam at 2.6 W average power. The beam profile remained the same at all amplifier diode current settings between 0 and 36 A.

Beam quality of the 1-pass output was measured using the same setup and method used for measuring microchip laser beam quality. The measured/fitted values were $M_x^2 = 1.00$ and $M_x^2 = 1.04$, which are essentially the same as for the microchip laser itself.

7. Two-pass amplifier performance

For 2-pass amplifier experiments, the 2-pass HR mirror of Fig. 7 is installed and the mirror is adjusted so the 2-pass output beam emerges from the slab at an angle relative to the input beam. The 2-pass beam was picked off with a flat HR mirror as shown. For the data reported here, no cylinder lens was present to re-collimate the vertical axis of the 2-pass output beam.

Fig. 10 shows *L–I* curves for the two-pass amplifier. A maximum output power of 5.7 W was achieved at a pulse rate of 10 kHz, resulting in pulse energy of 570 μJ, with a total pump power of 40 W at 36 A. Microchip laser power transmitted through the 2-pass amplifier with the amplifier off was about 114 mW.

The 2-pass amplifier was also evaluated with the microchip laser operating at pulse rates of 5 and 2 kHz. Pump power into the microchip was reduced to decrease microchip laser pulse rate. At 40 W total pump power in the amplifier, average output power was 3.3 W at 5 kHz (660 μJ per pulse) and 1.7 W at 2 kHz (850 μJ per pulse). To our knowledge, these numbers represent the highest pulse energies and average power levels reported to date from a single-amplifier microchip MOPA laser system.

Fig. 10 also shows how 2-pass output power changes as microchip laser power into the amplifier is varied. (The values shown are for microchip power transmitted through the 2-pass amplifier with the amplifier off). The half-wave plate before the isolator was rotated to adjust microchip power into the amplifier. Reducing microchip power by 50% reduced output power by 18%. A tenfold decrease in microchip laser input power reduced output power by only 48%.

A spatial profile of the 2-pass amplifier output beam is shown in Fig. 11. The beam is elongated in the vertical direction because no cylinder lens was used to re-collimate the vertical axis. Beam quality of the 2-pass amplified beam was measured using the same method as for the microchip laser and 1-pass-amplified beams. The fitted values were $M_x^2 = 1.01$ and $M_x^2 = 1.05$, which are essentially the same as for the microchip laser itself.

The isolator shown in Fig. 7 is required for 2-pass amplifier operation. Without the isolator, “four-pass ASE” can build up along the intended beam path as follows: backward-propagating spontaneous emission originating at the output end of the 2-pass amplifier makes two passes through the amplifier, reflects off the microchip

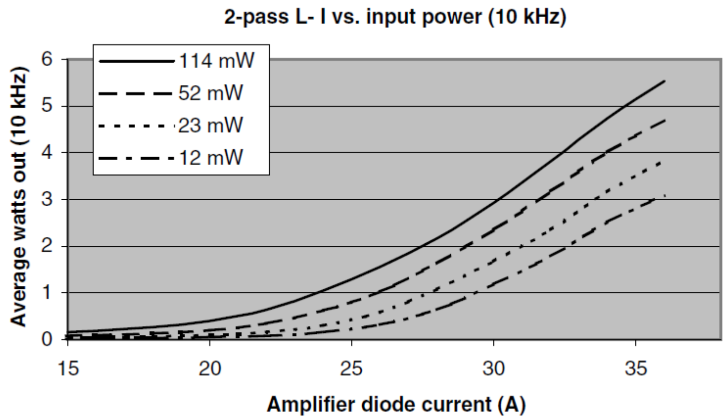

Fig. 10. Two-pass amplifier L–I curve at 10 kHz pulse rate for different values of microchip laser input power (different transmitted power levels when the amplifier is off).

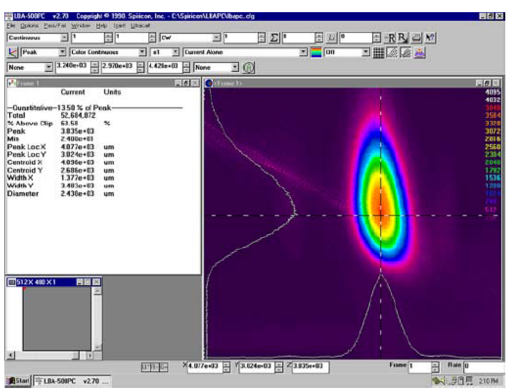

Fig. 11. Two-pass amplifier beam at 5.7 W out, 10 kHz pulse rate (no vertical collimator lens).

output coupler, and then makes another two passes through the amplifier in the forward direction. Nevertheless, significant power losses are avoided at the isolator since the isolator is not at the output end of the 2-pass amplifier, as would be the case if the isolator were needed to separate the input and 2-pass output beams. The isolator can be quite small and relatively inexpensive since the microchip laser beam is less than 1 mm in diameter at the isolator. Other isolation schemes that do not require a magneto-optic device, but throw away some of the oscillator emission, are rendered practical by the high gain achieved in the VHGM. (That is, high extraction efficiency can still be achieved in the VHGM even if some

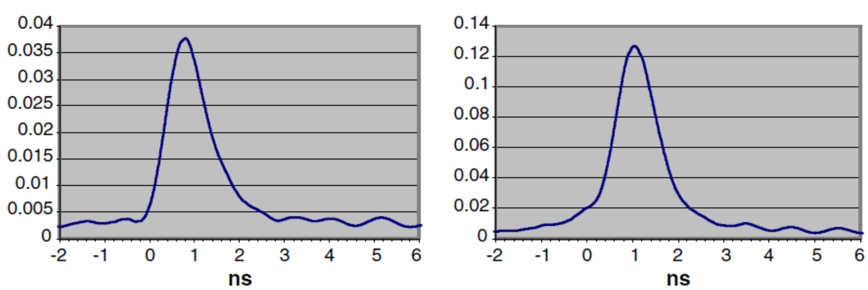

Fig. 12. Pulse shapes: (left) with amplifier off, and (right) with 2-pass amplifier on at 40 W pump power.

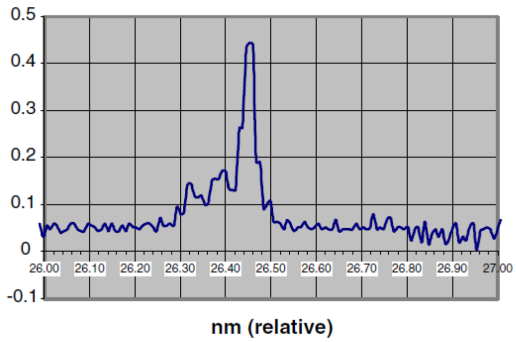

Fig. 13. Spectrum of 2-pass-amplified emission.

of the oscillator emission is discarded for the purposes of isolating the oscillator from the VHGM amplifier).

Temporal pulse shapes are shown in Fig. 12. Pulse duration for the 2-pass beam may be closer to 1.4 or 1.5 ns FWHM.

The spectrum of the 2-pass amplifier output is shown in Fig. 13. This shows that the isolator is doing a good job of preventing feedback or interaction between the amplifier and microchip oscillator that might increase the number of modes lasing in the microchip, or otherwise significantly alter the spectrum. These results suggest that the VHGM amplifier should preserve the spectrum of a true single-frequency microchip oscillator.

8. Conclusions

Long single-pass gain lengths enable the VHGM to act as an effective pre-amplifier when operated in 1-pass mode, and as an efficient power amplifier when operated in a 2-pass mode. With 40 W of total diode pump power, average output power levels in excess of 5.5 W have been demonstrated at pulse rates of 10 kHz, starting with less than 200 mW of microchip laser power. The VHGM amplifier preserves the TEMoo beam quality and emission spectrum of the microchip laser oscillator. We expect to achieve 10–15 W at 10 kHz when pumping with two 30 or 40 W diode bars.

When using Nd:YVO_4 as the gain medium, a VHGM-based amplifier should provide similar performance when used with other low-power TEMoo laser oscillators emitting at 1064 nm, possibly including certain types of diode lasers and fiber lasers. CW-pumping of a VHGM amplifier renders it suitable for amplifying a wide variety of cw and pulsed laser oscillators.

The complete microchip MOPA laser system can be made very compact. When pumping with 40 W of total diode pump power, it is expected that the laser can be packaged as a completely air-cooled system having no internal water-cooling loops. The pulse energies, pulse durations, and peak power levels provided are high enough to efficiently pump optical parametric amplifiers that employ periodically poled nonlinear materials.

Acknowledgements

The author acknowledges useful technical discussions with J.J. Zayhowski regarding microchip laser performance. The VHGM design, including variations thereof, is proprietary to JGM Associates, Inc. and is patent-pending.

References

[1] J.J. Zayhowski, Passively Q-switched picosecond microlaser, US Patent #5,394,413, 1995.
[2] J.J. Zayhowski, Rev. Laser Eng. 16 (1998) 841.
[3] J.J. Zayhowski, Miniature laser/amplifier system, US Patent #6,512,630, 2003.
[4] J.J. Zayhowski, Opt. Lett. 29 (2004) 1218.
[5] F. Druon, F. Balembois, P. Georges, A. Brun, OSA TOPS Adv. Solid-State Lasers 26 (1999) 134.
[6] Y. Isyanova, J.G. Manni, D. Welford, M. Jaspan, J.A. Russell, OSA TOPS Adv. Solid-State Lasers 50 (2001) 186.
[7] D.A.V. Kliner, F.D. Teodoro, J.P. Koplow, S.W. Moore, A.V. Smith, in: L.N. Durvasula (Ed.), Advances in Fiber Devices, Proceedings of the SPIE, vol. 4974, 2003, p. 230.
[8] T.M. Baer, High efficiency mode-matched solid-state laser with transverse pumping and cascaded amplifier stages, US Patent #5,271,031, 1993.